Article

Not peer-reviewed version

Power Drives Architectures for Industrial Hydraulic Axes: Energy Efficiency-based Comparative Analysis

Monica Tiboni *

Posted Date: 22 August 2023

doi: 10.20944/preprints202308.1379.v1

Keywords: energy efficiency; energy savings; industrial hydraulics; power drive architecture; CO2 emissions reduction

Article

Power Drives Architectures for Industrial Hydraulic Axes: Energy Efficiency-based Comparative Analysis

Monica Tiboni

Department of Mechanical and Industrial Engineering, University of Brescia,via Branze, 38, 25123 Brescia, Italy; monica.tiboni@unibs.it (M.T.)

Abstract: In hydraulic systems, energy dissipation can be significant. The pressure drops that can occur in the hydraulic circuit, influenced by the adopted drive architecture, result in an absorbed power often significantly greater than that required by the mechanical system. In this paper, a comparative study of energy efficiency among five drive common architectures in industrial hydraulic axes is carried out. The analysis is applied to a hydraulic blanking press with variable speed and force, a fairly frequent industrial system, e.g. in the production of semi-finished brass products. Standard, regenerative, high-low, variable displacement pump and variable speed drive for a fixed displacement pump configurations have been analysed and compared. An adequate and optimized sizing of the various components of the system has been carried out in each case and subsequently the energy consumption has been estimated for a load cycle common to all the considered cases. The results show that the choice of power generation architecture of the hydraulic system has a very significant impact on energy efficiency and consequently operating costs and carbon footprint. The performed quantification of the potential energy efficiency of the considered drive architectures can be very useful in guiding energy-conscious choices.

Keywords: energy efficiency; energy savings; industrial hydraulics; power drive architecture; CO_2 emissions reduction

1. Introduction

The global energy market is experiencing, in recent years, a considerable growth of request. This is accompanied by a significant increase in the sale and supply price and it is very likely that this trend will continue in the next years. The growing need for energy is manifested in its most striking form in the industrial field, where it is very frequent the execution of processes, of a different nature, with high or very high energy content. The more the power required by a process is high, the more important becomes the optimal selection of the drive technology of the machine used to perform the task. Typically, hydraulic technology is characterized by a high power density, much higher than that obtainable with pneumatic or electric drives. Therefore, the hydraulic technique is the preferential choice when the power involved in an industrial plant is high. In such circumstances, the economic savings deriving from the pursuit of high energy efficiency objectives is a corporate priority. Energy dissipation in hydraulic systems can be significant. The distributed pressure drops that can occur in the piping network or in the components of the hydraulic circuit determine upstream a pressure higher than that actually required by the actuators with a consequent increase in the absorbed power.

Furthermore, the chosen architecture for power generation has a very significant influence on the energy efficiency of the system. For example, in many systems a considerable amount of oil-hydraulic energy is dissipated between the inlet and outlet ports of the pressure relief valve, when dissipative speed adjustments of the actuators are obtained. This peculiarity of hydraulic technology clearly represents a factor that contributes to a fair degree of intrinsic inefficiency, but also determines a significant margin of potential for improvement that can be obtained through innovation. Therefore, hydraulic technology dedicated to the implementation and control of industrial machinery is a fertile ground in which to cultivate and develop design solutions characterized by an ever-increasing level of energy efficiency.

 doi:10.20944/preprints202308.1379.v1

For hydraulic applications in the industrial field or in the mobile applications, low energy consumption control systems and architectures that optimize overall efficiency have been studied and developed. Many auxiliary energy recovery circuits been investigated for hydraulic equipment. The most studied energy recovery circuits are based on accumulators, gas cylinder, gravitational potential energy, flywheel, generator super capacitor or generator-battery circuits. The hydraulic energy regeneration system (ERS) with the accumulator is excellent for machines that need to start and stop often, according to Tianliang et al. [1], who discussed several forms of ERS used in hydraulic construction gear.

Ho and Le in [2] presented a hydraulic system with high efficiency, which saves about 20% energy compared with systems without energy recovering. A high pressure hydraulic accumulator, a relief valve, an AC servo-motor, a fix displacement hydraulic pump, a hydraulic cylinder, seven directional controlled valves, a tank are the main components of the system. The method uses check valve to boost the pump using a low pressure accumulator as a tank. The flow direction to the pump is controlled by two check valves and the hydraulic cylinder velocity is regulated through the motor speed regulation. The high pressure accumulator boosts the pump and is used to store recovery energy. Due to the shifting algorithm of the valves, this system may operate in different configurations, allowing it to be flexibly modified to meet the desired operating requirements, such as high velocity, or torque but also high effectiveness of energy recovery from the load.

Niu et al. in [3] propose an innovative multifunctional energy-saving electro-hydraulic servo system. A servo-motor actuated the pump with a pressure regulation, two proportional valves and four switches, whose tuning allows to select three different control modes: single-valve independent control (SI), separate meter in and separate meter out control (SMISMO) and dual valve parallel control (DP). The supply pressure is controlled through a disturbance observer and the supply flow is controlled with a grey predictor. The experiments demonstrated supply pressure and flow loss reduction, and consequently an energy saving result.

In [4] Schmidt and Hansen introduce the concept of multi-cylinder/motor drives connection as a variable-speed drive network. Electrical and hydraulic interconnected variable-speed displacement units allow for the complete avoidance of throttle elements, while also for the sharing of auxiliary functions and fluid reservoirs, as well as hydraulic and electric power.

Xu et al. in [5] presented an analytical technique based on the mathematical energy dissipation model of hydraulic components in order to calculate the system energy dissipation by creating a high precision simulation model. They applied the method to a 10000 kN fine blanking press.

Similarly, in order to identify the cause of the low energy efficiency in large and medium-sized hydraulic presses, Zhao et al. [6] suggested an analytical method for quantifying energy flow in the system. Starting from the basic formula of energy consumption, they identified a limited number of unknown coefficients, whose values can be estimated through experiments.

Based on an investigation of the energy flow characteristics of the hydraulic system, Li et al. [7] proposes an energy-saving strategy by balancing the load of press operations. The method involves sharing the drive system's motor pumps at different times with a unit made up of two hydraulic presses in order to minimize energy loss during unloading activities. These two presses are also coupled, and during some operations the extra energy from one press can be used as the input energy for the other one to increase the efficiency of the drive system. Additionally, the potential energy can also be used directly. To provide energy for both hydraulic presses, the drive systems of two of them are merged into one (combined drive system, CDS). Presses 1 and 2 get energy at certain times from each motor-pump in the combined drive system, and each motor-pump is separately controlled.

A Direct Driven Pump-controlled hydraulic system (DCP), characterized by a closed circuit type, a speed-controlled electric servomotor and a fixed displacement pump, was studied by Koitto et al. [8] for a stationary industrial material-handling application that consecutively lifts and lowers a fixed mass. The energy savings ranged from 53 to 87% when compared to a conventional valve-controlled approach. Although the actuator tended to vibrate when it reached the desired position and the system

 doi:10.20944/preprints202308.1379.v1

pressures oscillated strongly during the movement of the cylinder, the dynamics of the system did not quite fulfil the stated requirements.

Remaining in the industrial field, studies aimed at increasing energy efficiency have also been conducted for hydraulic injection molding machines (HIMMs). The clamping force control (FC) demands high pressure but low volume flow, requiring just a little amount of power. The widespread hydraulic valve-controlled cylinder systems, which set the maximum supply pressure with a relief valve and constant displacement pumps, offer good servo control response but poor energy efficiency. To increase the energy efficiency, energy-saving control methods based on an electro-hydraulic variable-displacement pump system (EHVDPS), such as load-sensing control (LSC) and constant supply pressure control (CSPC) are used. From the studies of Chiang et al. [9] emerged that the energy consumptions of (FC + LSC) and (FC + CSP) are 17.9 and 67.4% of the input energy of the EHVDPS method, respectively.

System power consumption can also be an indicator of operating conditions. In particular, application-independent variations in energy consumption can be related to malfunctions in the hydraulic system [10–14]. Condition monitoring techniques based on artificial intelligence algorithms can be used to prevent any system malfunctions.

There are many solutions investigated at the research level, but these are rarely used in the industrial field. However, there are some solutions that are typically applied in the industrial field, some historical and some much more recent, for which, however, comparative studies in energy terms are not reported in the literature.

Analytical modelling of all the phenomena involved in the operation of an oil-hydraulic drive architecture to estimate the overall efficiency is complex [15]. Distributed and concentrated pressure drop, fluid viscosity fluctuations due to temperature variations, influence of fluid viscosity, pressure and rotational speed on the pump volumetric and the hydro mechanical efficiencies, valve switching delay, active and reactive electric current components absorbed by the power supply (influenced by the rotational speed), dynamic friction between the piston and the cylinder body are some of the multiple factors which affect functioning and efficiency of an hydraulic system.

An estimate of the energy efficiency and of the impact of energy consumption on operating costs for different plant architectures is information of significant use in the design of these plants. In the present discussion a comparative study is carried out in terms of energy efficiency among different architectural solutions for the power part of a hydraulic blanking press with variable speed and force, a very common industrial process, e.g. in the production for semi-finished brass products. The volumetric flow rate and pressure of a fluid change over time in a process with varying speed and force, and it is under these operating conditions that the various technological solutions that can be used for the power part are distinguished by significantly different levels of energy efficiency.

The energy dissipations that distinguish one solution from another were examined in the analysis, while ignoring the contributions that are shared by all solutions.

The analysis is applied to a specific industrial process, in detail pressing of semi-finished brass products. Different hydraulic architectures will be presented, all equally capable of meeting the required performance, discriminated, however, by a progressively higher level of energy efficiency. The different configurations analyzed, starting from a traditional hydraulic architecture of low energy efficiency, are characterized by the introduction of the regenerative technique and variations in the unit for converting electrical energy into hydraulic energy carried by the fluid under pressure.

Five configurations, whose architecture is described below and summarized in Table 1, have been analyzed and compared.

1. Standard configuration: traditional architecture consisting of a round-case induction electric motor, a fixed displacement vane pump, a pressure relief valve, and a standard directional control valve (DCV);
2. Regenerative configuration: standard configuration with DCV with regeneration A – Hybrid;

 doi:10.20944/preprints202308.1379.v1

3. High - Low configuration: regenerative A – Hybrid configuration in which the single fixed-displacement vane pump is replaced by two pumps of the same type, one with high flow rates and low maximum pressures, one with low flow rates and high maximum pressures;
4. VDP (Variable Displacement Pump) configuration: regenerative A – Hybrid configuration in which the single fixed displacement vane pump is replaced by a variable displacement axial piston pump;
5. DCP (Drive Controlled Pump) configuration: regenerative A – Hybrid configuration in which rotational speed of the asynchronous motor is continuously adjustable through an AC frequency converter.

Table 1. Considered and compared power drive architectures for a press for semi-finished brass products.

Configuration	Electric Drive	Pump	Directional Valve
Standard	round-case induction electric motor	fixed displacement vane pump	standard DCV
Regenerative	round-case induction electric motor	fixed displacement vane pump	DCV with regeneration A – Hybrid
High - Low	round-case induction electric motor	two fixed-displacement vane pumps	DCV with regeneration A – Hybrid
VDP	round-case induction electric motor	variable displacement axial piston pump	DCV with regeneration A – Hybrid
DCP	AC frequency converter + round-case induction electric motor	fixed displacement vane pump	DCV with regeneration A – Hybrid

For a quantitative comparison of the energy efficiency performance of the examined configurations, it is necessary, for each of them, to carry out the selection an optimized sizing of the main components.

For configurations 1 to 4, the sizing can be done by neglecting the angular acceleration or deceleration ramps that characterize the transition from one speed regime to another, because in architectures that adopt an asynchronous motor powered directly from the power grid, the inertial torques resulting from the acceleration or deceleration ramps can in first approximation be neglected. On the other hand, the contribution of inertial torques becomes more relevant when the motor is fed through a frequency converter, because in this mode of operation the motor is subject to excursions in speed of very large amplitude even in very short times, resulting in non-negligible inertia torques. For architecture 5, both an approximate sizing, neglecting the inertial contribution, and a more accurate sizing, also taking into account the inertial contribution, was carried out.

2. Materials and Methods: Architectural Configurations for the Case Study

This section is dedicated to the description of the characteristics of the considered solutions for a case study that refers to a real application. In detail, the following will be introduced: the structure and the parameters of the process considered as case study, the technical requirements, the elements that are common to all the analyzed cases, i.e. actuator and fluid, the theoretical analysis adopted to estimate physical quantities necessary for sizing the system, the procedures adopted for the selection and sizing of the circuit components, and, lastly, all the final configurations of the considered architectures, reported in Table 1.

2.1. The Hydraulic System

This section describes the main characteristics of the hydraulic system under analysis. First, the structure of the system is described and the technical specifications considered for conducting the quantitative analysis are identified, then the technical data of the circuit elements that are common to all the considered configurations are reported.

Preprints (www.preprints.org) | NOT PEER-REVIEWED | Posted: 22 August 2023 doi:10.20944/preprints202308.1379.v1

2.1.1. System Structure and Technical Requirements

The main technical requirements for the actuator during operation are two: the minimum thrust force that the rod must exert during the blanking of the semi-finished product and the maximum duration of the entire work cycle of the press. The solution for the pressing of semi-finished brass products considered as a case study is composed of an hydraulic press with a piece feeding/unloading system that includes a rotary table with four stations, a robot manipulator and a conveyor belt, as shown in Figure 1.

The typical blanking work cycle is divided into two macro phases. The first includes the rod quick descent, the blanking, the expulsion of the piece and the rode quick rise. In this first macro phase the cylinder is actively involved in the work cycle. The second, on the other hand, involves only the rotation of the table for loading the parts to be machined. In this case the cylinder rod does not perform any movement and remains in a waiting condition. The duration of this second macro phase is normally bound by the end user of the machine and in the process considered as a case study it is equal to 0.3 s. It is therefore evident that the constraint on the maximum duration of the blanking cycle determines a limitation to the maximum duration of the first macro phase, in which the cylinder is in motion. In addition to the constraints on the minimum force to be produced in operation and on the maximum duration of the work cycle, a third limitation is set. This defines the limiting mass of the tooling that can be anchored to the free end of the actuator stem. The numerical values of the above parameters are summarized in Table 2.

Figure 1. Pressing system considered as a case study and main constituent elements.

Table 2. Technical requirements for the hydraulic system.

Parameter	Value	Unit
Minimum blanking force	294300	[N]
Rotation phase duration for the rotary table	0.3	[s]
Maximum duration of the entire processing cycle	1.4	[s]
Maximum duration of operation for the actuator	1.1	[s]
Maximum mass of the tooling anchored to the rod	80	[kg]

Preprints (www.preprints.org) | NOT PEER-REVIEWED | Posted: 22 August 2023 doi:10.20944/preprints202308.1379.v1

There are five individual phases involved in the whole process: Quick Descent (QD), Blanking (B), Expulsion (E), Quick Rise (QR) and Table Rotation (TR). During the blanking phase, pressure and speed have a fairly complex trend, which should be identified either experimentally or by simulating the process. For the purposes of this work, i.e. the functional comparison between the different system architectures for energy efficiency, the influence of the variation of these two quantities in the blanking phase on the overall energetic consumption values is limited. The discussion is therefore conducted in the simplified hypothesis that the speed on the load is uniform, with a value equal to the average one during the cutting operation and that the pressure of the oil is constant and equal to the maximum value reached in blanking.

Table 3 shows the values of the rod stroke and of the pressure at the delivery of the pumping group for the phases of blanking cycle. Figure 2 shows the Cyclogram of the work phases, obtained by considering a periodic cyclic load with negligible dynamics on the actuator.

Table 3. Rod stroke, piston translation speed, maximum pressure and maximum flow rate in the processing cycle phases.

Parameter	Unit	Quick Descent - QD	Blanking - B	Expulsion - E	Quick Rise - QR	Table Rotation - TR
stroke (s)	[mm]	40	20	20	80	-
velocity (v)	[mm/s]	250	67	67	250	-
max. pressure (P)	[bar]	50	200	70	70	10
max. flow rate (Q)	[l/min]	230.8	61.9	61.9	13	10

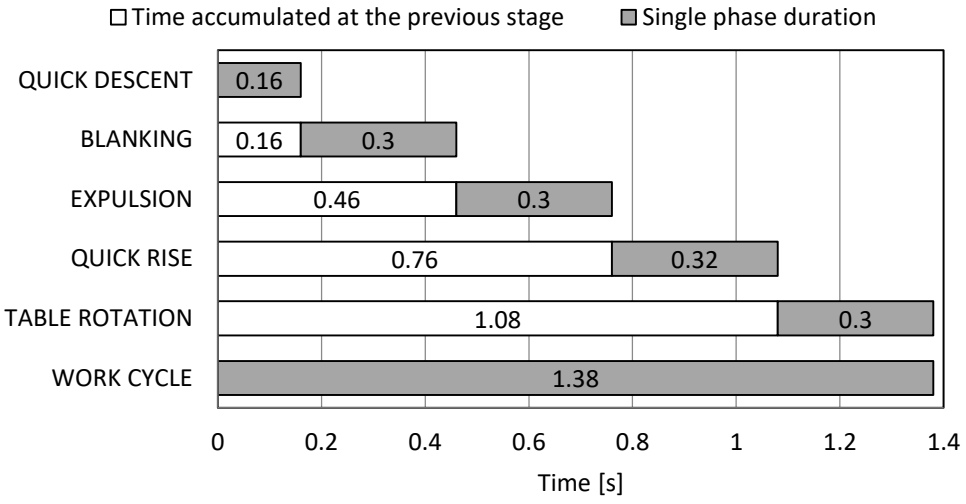

Figure 2. Cyclogram with periodic cyclic loading at negligible dynamics.

The dynamic effects at the shaft of the electric motor are much more relevant. For architectures in which the three-phase asynchronous motor is connected directly to the electrical network, the motor maintains a rotation speed belonging to a neighborhood of the rated speed. The only deviations from the nominal speed value, excluding the starting and stopping phases, are caused by the phenomenon of motion irregularity, due to the periodicity of the load. The amplitude of the excursion made by the rotation speed is very low, resulting in the possibility to neglect the inertial effects on the crankshaft. For the DCP architecture in which an inverter is used, considering the overall cycle time of 1.4 s, it is evident that the acceleration and angular deceleration ramps cause inertial torques to the motor shaft that must be taken into consideration. In summary, the inertial aspects of the crankshaft can be neglected in the sizing of Standard, High - Low and VDP architectures. Instead, they must be taken into account when sizing the architecture with DCP.

Preprints (www.preprints.org) | NOT PEER-REVIEWED | Posted: 22 August 2023 doi:10.20944/preprints202308.1379.v1

2.1.2. Hydraulic Cylinder and Fluid

Figure 3 reports the flow-chart of the cylinder sizing process, and for the circuit elements common to all configurations, the fluid and the cylinder, the designations and related technical characteristics of the chosen types are listed in Table 4.

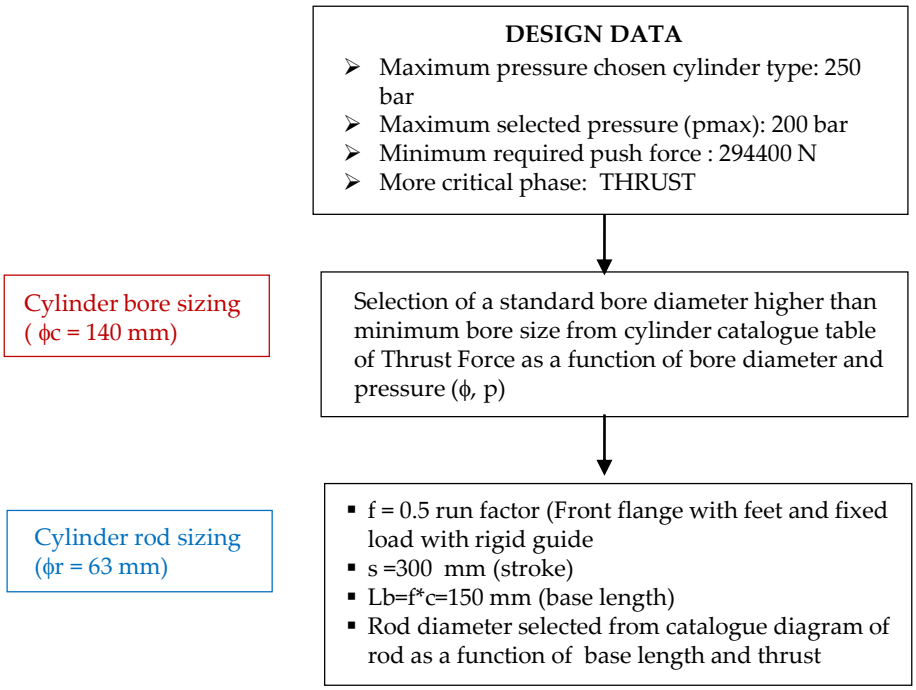

Figure 3. Flow-chart of cylinder sizing.

Table 4. Fluid and cylinder: designations and technical data.

Circuit Element	Parameter	Value
Fluid	Code	Castrol serie HYSPIN ZZ 46
	Fluid Type	Mineral Oil
	Viscosity	ISO VG 46
Cylinder	Code	Parker 140MF3MMAXRN23M300M1133AOAO
	Type	Double Acting
	Bore	140 [mm]
	Rod Diameter	100 [mm]
	Stroke	300 [mm]
	Fixing	Front flange with feet and fixed load with rigid guide
	Area Ratio	1.96

2.1.3. Theoretical Analysis of a Valve Controlled Circuit

For the system sizing actual forces and speeds are required, and consequently pressures and flow rates. This paragraph provides the theoretical analysis necessary for calculating these quantities.

The simplest control circuit that can be used for a linear actuator combines the differential cylinder with an area ratio of $2:1$ with a standard $1:1:1:1$ directional control valve. Let adopt the Nomenclature reported in Figure 5: the flow rate through the rear chamber and the flow rate through the front chamber of the actuator are respectively defined with Q_A and Q_B. p_A and p_B denote the relative pressures which occur respectively in the rear and front chambers of the cylinder. p_P is the pressure that is established at the delivery of the pumping unit. The fluid pressure in the supply and discharge tank is indicated with p_T. Since, in general, the oil pressure inside the tank is equal to the atmospheric pressure, the pressure p_T, being a value relative to the atmospheric pressure, is assumed zero. For a differential cylinder the Area Ratio α is defined as $\alpha = \frac{A_P}{A_T}$ and the flow rates relating to the two chambers in the exit stroke have the expressions reported in eq. 1.

Preprints (www.preprints.org) | NOT PEER-REVIEWED | Posted: 22 August 2023 doi:10.20944/preprints202308.1379.v1

In the 4-port used directional valve (P=pressure, T=discharge, A=first port; B=second port) the indication 1:1:1:1 means that for the ways AT: PA: PB: BT the drop of pressure is equal to Δp_n when 100% of the nominal flow ΔQ_npasses through it. 1 stands for 100%, a different value means a different percentage, e.g 0.5 for 50%.

In the following of the discussion, the pressure drops on the DCV, the pressures that are realized in the rear and front chambers of the cylinder, the push and pull forces that can be exercised by the rod and the maximum speed that it can reach during the outward and return phases will be determined, at a theoretical level. In the analysis, both the pressure and the rod translation speeds, relative to the exit strokes and return, will be assumed constants. To distinguish the parameters referring to the outward stroke from the parameters referring to the inward stroke, the apexes "o" (outward) and "i" (inward) will be used.

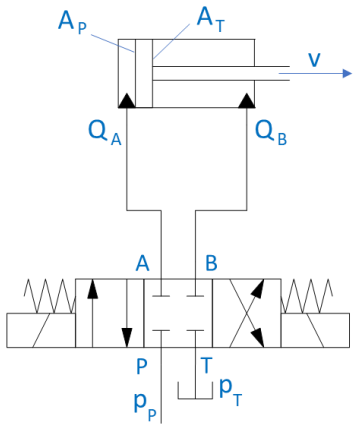

Figure 4. Symbols for theoretical analysis of the system.

$$Q_A^o = vA_P \qquad Q_B^o = \frac{Q_A^o}{\alpha} \tag{1}$$

The relationship between the flow rate that crosses a DCV way and the pressure drop that occurs on the way itself is expressed by eq. 2.

$$Q_x = Q_n \sqrt{\frac{\Delta p_x}{\Delta p_n}} \tag{2}$$

Consequently, the pressure drops on the PA and BT ways can be expressed as reported by eqs. 3 and 4.

$$\Delta p_{PA} = p_P - p_A^o = \Delta p_n \left(\frac{Q_A^o}{Q_n}\right)^2 = \Delta p_n \left(\frac{vA_p}{Q_n}\right)^2 \tag{3}$$

$$\Delta p_{BT} = p_B^o - p_T = p_B^o = \Delta p_n \left(\frac{Q_B^o}{Q_n}\right)^2 = \Delta p_n \left(\frac{vA_P}{\alpha Q_n}\right)^2 \tag{4}$$

For a cylinder with area ratio 2, the ratio between the pressure drops between ports P and A and B and T is $\frac{\Delta p_{PA}}{\Delta p_{BT}} = \alpha^2 = 4$. From eqs. 3 and 4, the pressures in the rear and front chambers of the actuator can be derived (eqs. 5 and 6).

$$p_A^o = p_P - \Delta p_n \left(\frac{vA_p}{Q_n}\right)^2 \tag{5}$$

$$p_B^o = \Delta p_n \left(\frac{vA_P}{\alpha Q_n}\right)^2 \tag{6}$$

Preprints (www.preprints.org) | NOT PEER-REVIEWED | Posted: 22 August 2023 doi:10.20944/preprints202308.1379.v1

The thrust force created by the rod is expressed by eq.7.

$$F^o = p_A^o A_P - p_B^o \frac{A_P}{\alpha} = p_P A_P - A_P \Delta p_n \left(\frac{v A_P}{Q_n}\right)^2 - \frac{A_P}{\alpha} \Delta p_n \left(\frac{v A_P}{\alpha Q_n}\right)^2 \tag{7}$$

With reference to the inward movement, the analysis procedure is similar to that used for the outward one, obtaining flow rates, pressure drops on the valve ways and pressures in the cylinder chambers as reported in the eqs. 8, 9, 10, 11, 12.

$$Q_B^i = v A_T = \frac{v A_P}{\alpha} \qquad Q_A^i = \alpha Q_B^i = v A_P \tag{8}$$

$$\Delta p_{PB} = p_P - p_B^i = \Delta p_n \left(\frac{Q_B^i}{Q_n}\right)^2 = \Delta p_n \left(\frac{v A_p}{\alpha Q_n}\right)^2 \tag{9}$$

$$\Delta p_{AT} = p_A^i - p_T = p_A^i = \Delta p_n \left(\frac{Q_A^i}{Q_n}\right)^2 = \Delta p_n \left(\frac{v A_P}{Q_n}\right)^2 \tag{10}$$

$$p_B^i = p_P - \Delta p_n \left(\frac{v A_p}{\alpha Q_n}\right)^2 \tag{11}$$

$$p_A^i = \Delta p_n \left(\frac{v A_P}{Q_n}\right)^2 \tag{12}$$

In inward phase the ratio between the pressure drops between ports P and B and A and T is $\frac{\Delta p_{BT}}{\Delta p_{AT}} = \frac{1}{\alpha^2} = \frac{1}{4}$.

During the retraction phase, the stem exerts a pulling action. This force is expressed by eq. 13.

$$F^i = p_B^i A_T - p_A^i A_P = p_B^i \frac{A_P}{\alpha} - p_A^i A_P = \frac{p_P A_P}{\alpha} - \frac{A_P}{\alpha} \Delta p_n \left(\frac{v A_P}{\alpha Q_n}\right)^2 - A_P \Delta p_n \left(\frac{v A_P}{Q_n}\right)^2 \tag{13}$$

With v and p_p being equal, the thrust force is greater than the pulling force. Both in the exit and retraction phases, the maximum force value is obtained for $v = 0$. In this case the ratio between F^o and F^i is equal to α.

$$\left.\frac{F^o}{F^i}\right|_{v=0} = \alpha \tag{14}$$

If Q_P is the effective flow rate delivered by the pumping group, the maximum translation speed of the rod during the output stroke is the minimum value between the one obtained from eq. 1 setting $Q_A^o = Q_P$ and the one that derives from setting F^o equal to zero.

$$v_{max}^o = \min \left\{ \frac{Q_P}{A_P}, v|_{F^o=0} = \sqrt{\frac{p_P}{\frac{\Delta p_n A_p^2}{Q_n^2}\left(1 + \frac{1}{\alpha^3}\right)}} \right. \tag{15}$$

Similarly, the maximum translation speed of the rod during the return stroke is the minimum value between the one obtained from eq. 8 by setting $Q_B^i = Q_P$ and the one resulting from setting equal to zero the force F^i.

$$v_{max}^i = \min \left\{ \frac{Q_P}{A_T}, v|_{F^i=0} = \sqrt{\frac{\frac{p_P}{\alpha}}{\frac{\Delta p_n A_p^2}{Q_n^2}\left(1 + \frac{1}{\alpha^3}\right)}} \right. \tag{16}$$

Preprints (www.preprints.org) | NOT PEER-REVIEWED | Posted: 22 August 2023 doi:10.20944/preprints202308.1379.v1

Regeneration is typically performed during the rod out stroke, and consists in directing the flow of oil expelled from the anterior chamber of the actuator, as a consequence of the translation motion of the piston, inside the sleeve of the rear chamber cylinder. This results in a sensitive energy saving, which is why architectures that adopt DCVs with regeneration are called economizer circuits.

In the proposed study, the point of reinsertion of the fluid is located downstream of the PA way, i.e. towards the user, therefore the Regeneration is type A, and specifically A - Hybrid.

The configuration with Regeneration A - Hybrid integrates in the valve body the functions of a non-return valve on the BA line and an On - Off valve on the connection between point A and the tank. These two functions allow, during the outfeed stroke, to pass from a configuration with Internal Regeneration – A to a Standard configuration. In this way it is possible to have, if necessary, both the advantages of Internal Regeneration - A (energy efficiency) and the advantages deriving from the Standard configuration (high forces).

The analysis of flow rates, pressures, speeds and forces for the outward stroke in the case of Regeneration A - Internal follows (eqs. 17,18,19,20,21), in a similar way to what was done for the standard configuration.

$$\Delta p_{PA} = p_P - p_A^o = \Delta p_n \left(\frac{Q_P}{Q_n}\right)^2 \qquad p_A^o = p_P - \Delta p_n \left(\frac{Q_P}{Q_n}\right)^2 \tag{17}$$

$$\Delta p_{BA} = p_B^o - p_A^o = \Delta p_n \left(\frac{Q_B^o}{Q_n}\right)^2 = \Delta p_n \left(\frac{vA_P}{\alpha Q_n}\right)^2 \quad p_B^o = p_P - \Delta p_n \left(\frac{Q_P}{Q_n}\right)^2 + \Delta p_n \left(\frac{vA_P}{\alpha Q_n}\right)^2 \tag{18}$$

$$F^o = p_P A_P \left(1 - \frac{1}{\alpha}\right) - A_P \Delta p_n \left(1 - \frac{1}{\alpha}\right) \left(\frac{Q_P}{Q_n}\right)^2 - \frac{A_P}{\alpha} \Delta p_n \left(\frac{vA_P}{\alpha Q_n}\right)^2 \tag{19}$$

$$F^o = p_P A_P \left(1 - \frac{1}{\alpha}\right) - A_P \Delta p_n \left(\frac{vA_P}{\alpha Q_n}\right)^2 \tag{20}$$

$$v|_{F^o=0} = \sqrt{\frac{p_P \left(1 - \frac{1}{\alpha}\right)}{\frac{\Delta p_n A_P^2}{Q_n^2 \alpha^2}}} \tag{21}$$

Using regeneration, the maximum push force that can be exerted during rod extension is only half of that which can be produced using a standard circuit. From a constructive point of view, the DCV used for Regeneration - A Hybrid integrates the functions of non-return valve and On - Off valve in its upper part. The connections between the DCV and the branches of the hydraulic circuit, located in the part bottom of the valve body, remain unchanged compared to those found in a DCV Standard. This allows the modernization of an existing hydraulic drive, increasing its energy efficiency through the introduction of the regeneration technique, simply by replacing the body of a traditional directional control valve.

2.2. Standard Configuration

The main elements of the Standard Architecture are: the actuator, a three-phase 4-pole asynchronous motor with a round case connected directly to the electrical network, a fixed displacement vane pump, with a maximum pressure on the discharge port of 320 bar, a 1: 1: 1: 1 DCV standard directional valve and a pilot operated proportional pressure relief valve. The power source part of the Standard Configuration is shown in Figure 5.

Preprints (www.preprints.org) | NOT PEER-REVIEWED | Posted: 22 August 2023 doi:10.20944/preprints202308.1379.v1

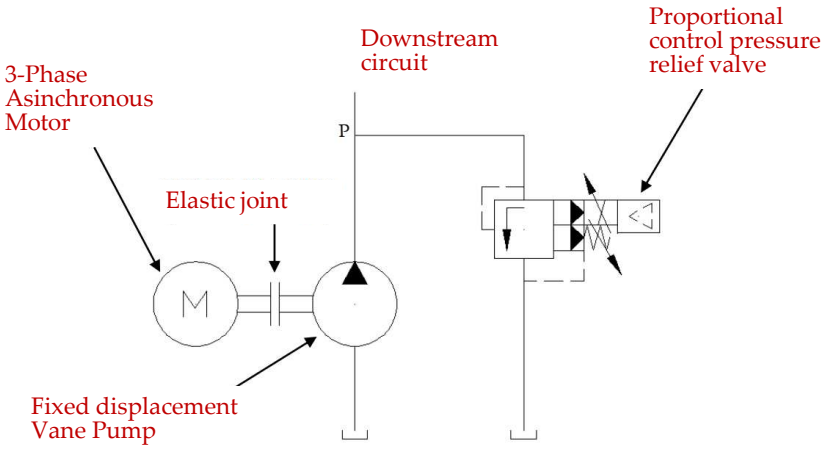

Figure 5. Standard Architecture power source scheme.

The flow-chart of the system sizing procedure for the standard configuration is reported in Figure 6. For the other configurations a similar sizing approach is followed.

Chosen the motor and pump types (in this case a 4 pole 3-phases asynchronous motor and a fixed vane pump), a first attempt dimensioning of the electric motor and the pump is carried out. The theoretical flow rate of the pump Q_{th} must be higher than the flow rate required by the load in the most critical condition. The nominal power of the electric motor must be higher than the mean power required in the cycle by its load, which is the pump. In the case of an asynchronous drive directly connected to the grid, the rotation speed of the motor is very close to the nominal speed. For the direct connection between motor and pump, motor and pump speeds are equal. Knowing the speed and the theoretical flow rate of the pump, it is possible to calculate the minimum pump displacement, and the pump can be chosen (respecting the minimum displacement, the maximum speed and the maximum pressure limitations). Having determined the effective flow rate of the pump (by subtracting the losses due to leakage from the theoretical one), it must be verified that this is sufficient in all operating conditions. If the verification is satisfied, proceed, otherwise a different pump size must be chosen. The directional valve and the maximum pressure valve are then sized. The first on the basis of the effective flow that passes through it and on the pressure drops between its ways in relation to the degree of opening; the second on the basis of the regulation pressure estimate, which depends on the characteristic (opening pressure $p_{opening}$, discharged flow $Q_{discharged}$). Finally, the torque that the engine must deliver must be checked. The rated torque of the motor must be greater than the root mean square value of the torque required in the cycle. The estimation of pressures and flow-rates (according the theoretical approach reported in Section 2.1.3 is needed for the procedure application.

Table 5 shows the most significant technical data of the chosen components, Figure 7 the main components, and Figure 8 the active electrical power absorbed in the cycle for the Standard Configuration.

Preprints (www.preprints.org) | NOT PEER-REVIEWED | Posted: 22 August 2023 doi:10.20944/preprints202308.1379.v1

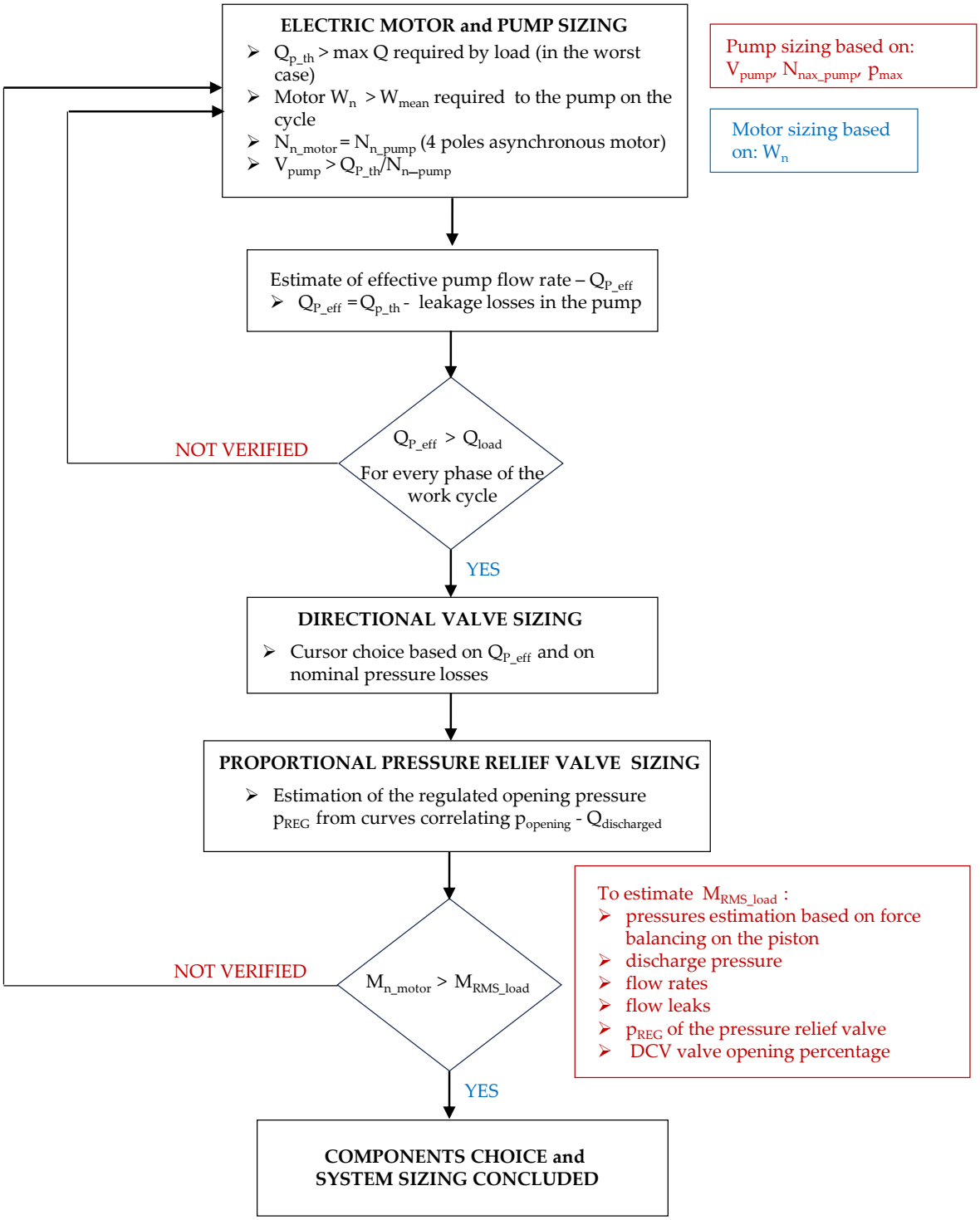

Figure 6. Standard Architecture: system sizing flow chart.

Preprints (www.preprints.org) | NOT PEER-REVIEWED | Posted: 22 August 2023 doi:10.20944/preprints202308.1379.v1

Table 5. Designations and technical data of the main elements of the standard architecture.

Circuit Element	Parameter	Value
Electric motor	Code	Parker Mod. MR4P05500
	Type	4 poles - round case
	Nominal Power	55 [kW]
	Nominal Speed	1480 [RPM]
	Nominal Torque	354.87 [Nm]
	Efficiency	0.935
Pump	Code	Parker Mod. T7E 050
	Type	Fixed Displacement Vane Pump
	Nominal Displacement	158.5 [ml/min]
	Speed Range	600 - 2200 [RPM]
	Max continuous pressure	210 [bar]
Directional Valve	Code	Parker Mod. D41FEE02FC1NB70
	Type	Pilot operated Proportional DCV 1:1:1:1
	Nominal flow rate	200 [l/min]
	Nominal pressure drop	5 [bar]
Pressure Relief Valve	Code	Parker Mod. R4V03535P0PM10VA1
	Type	Pilot operated proportional pressure relief valve
	Nominal flow rate	250 [l/min]
	Maximum Pressure	350 [bar]

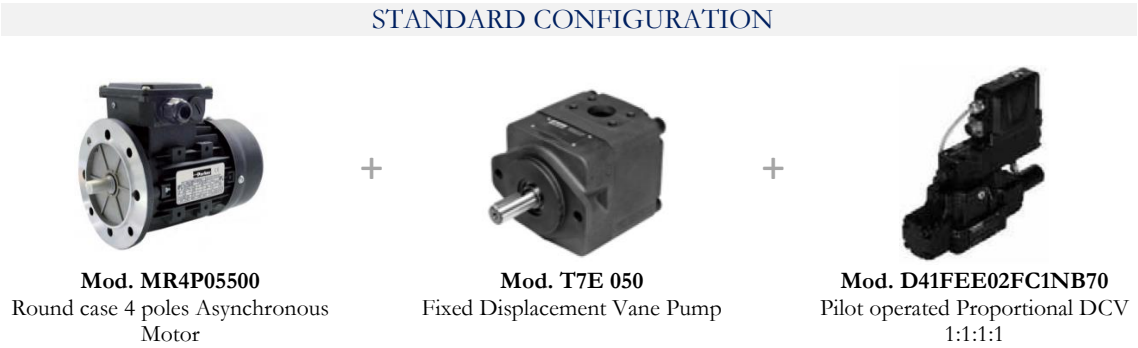

Figure 7. Main components of the Standard Configuration.

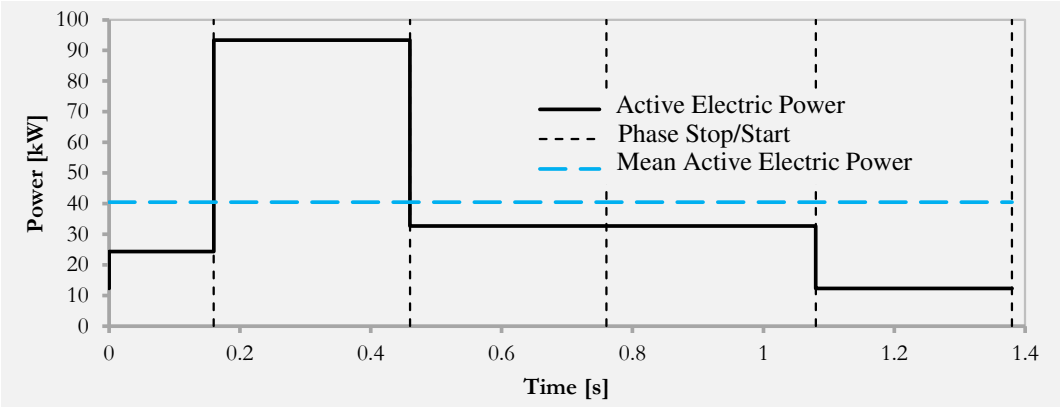

Figure 8. Standard Configuration - Active electrical power absorbed over the work cycle: instantaneous value and average value.

2.3. Regenerative Configuration

The regenerative configuration differs from the Standard one for the introduction of the regenerative function in the Rapid Descent phase, i.e. when a higher amount of flow is required. The DCV valve that is used allows a new path to be followed by the flow of oil leaving the actuator rod side chamber, the BA path, and this internal path allows regeneration. Therefore, a valve with Regeneration A - Hybrid is chosen which allows the introduction of Regeneration - A (Figure 9) during the phase in which the stem requires a high speed of translation in output, and to pass to the Standard

Preprints (www.preprints.org) | NOT PEER-REVIEWED | Posted: 22 August 2023 doi:10.20944/preprints202308.1379.v1

configuration when the stem is required to realize considerable pushing force. Table 6 shows the characteristics of the components used in this configuration. The regenerative function allows to significantly decrease the flow rate that must be delivered by the pump in the rapid descent phase: with regeneration the value is 117 l/min, compared to the 230.8 l/min required without regeneration. Consequently, the motor and electric and pump sizes are significantly reduced, as can be seen from the comparison between data in Table 6 and in Table 5.

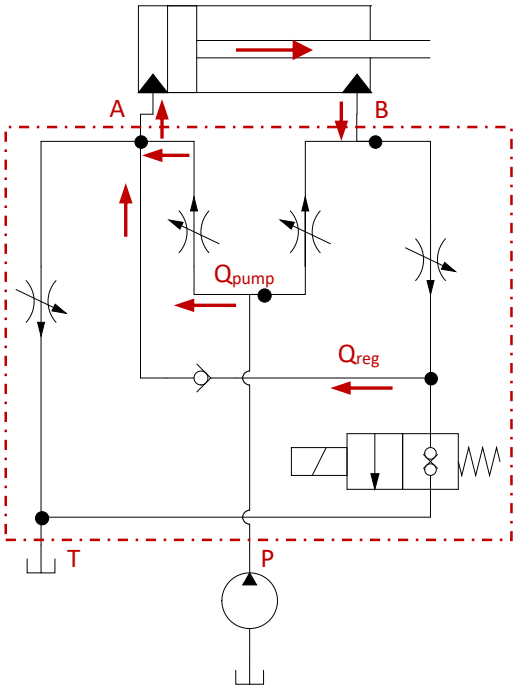

Figure 9. Active regeneration for high-speed movement.

Table 6 shows the most significant technical data of the chosen components, Figure 10 the main components, and Figure 11 the active electrical power absorbed in the cycle for the Regenerative A - Hybrid Configuration.

Table 6. Designations and technical data of the main elements of the regenerative architecture.

Circuit Element	Parameter	Value
Electric motor	Code	Parker Mod. MR4P03000
	Type	4 poles - round case
	Nominal Power	30 [kW]
	Nominal Speed	1460 [RPM]
	Nominal Torque	196.22 [Nm]
	Efficiency	0.923
Pump	Code	Parker Mod. Mod. T7D B24
	Type	Fixed Displacement Vane Pump
	Nominal Displacement	81.1 [ml/min]
	Speed Range	600 - 3000 [RPM]
	Max continuous pressure	250 [bar]
Directional Valve	Code	Parker Mod. D41FEZ32FC1NB70
	Type	Pilot operated Proportional DDCV with Regeneration - A Hybrid
	Nominal flow rate	200 [l/min]
	Nominal pressure drop	5 [bar]
Pressure Relief Valve	Code	Parker Mod. R4V03535P0PM10VA1
	Type	Pilot operated proportional pressure relief valve
	Nominal flow rate	250 [l/min]
	Maximum Pressure	350 [bar]

Preprints (www.preprints.org) | NOT PEER-REVIEWED | Posted: 22 August 2023 doi:10.20944/preprints202308.1379.v1

Figure 10. Main components of the Regenerative A - Hybrid Configuration.

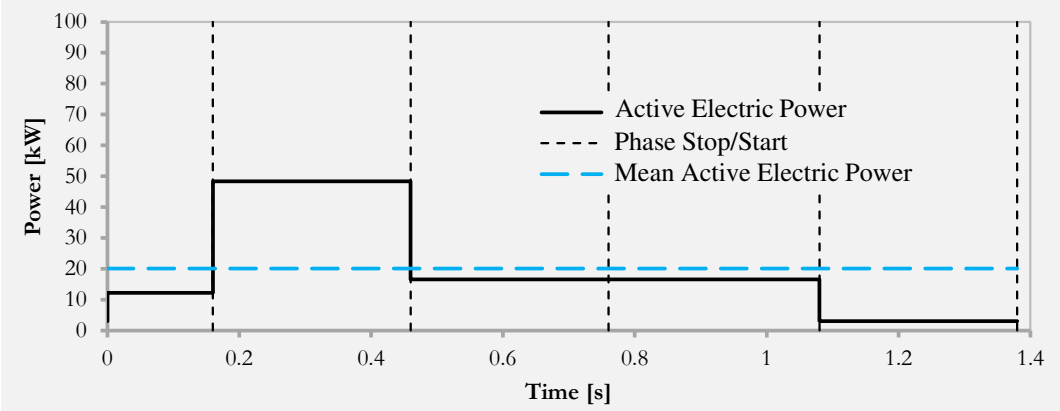

Figure 11. Regenerative A - Hybrid Configuration - Active electrical power absorbed over the work cycle: instantaneous value and average value.

2.4. High-Low Configuration

The High - Low architecture allows a generation of hydraulic power that varies over time. The generation of hydraulic power is divided into two distinct phases, such as the output stroke of the rod, and satisfies the variable needs of the user instead of looking only at the heaviest operating condition. The first phase of power generation takes place during the Rapid Descent, the second during the Blanking. The production of hydraulic power is therefore divided between a period in which a high flow rate of oil at relatively low pressure is required, and a period in which the demand for flow rate of fluid is reduced, accompanied by an increase in pressure. The designation High - Low is due to this alternation of operating conditions, to which the power generation must adapt. This architecture is very well suited to the blanking process performed by the press. In Figure 12 the circuit diagram of the power generation part for the High - Low architecture is reproduced. The system consists of two fixed displacement vane hydraulic pumps. The pumps are operated by a single round case asynchronous motor directly connected to the power supply network and have opposite hydraulic characteristics. A pump has a relatively low maximum operating pressure limit and high displacement, and it is called LPHD (Low Pressure High Displacement). The other pump is characterized by a high value of the maximum operating pressure limit and by a relatively low displacement, and it is defined as HPLD (High Pressure Low Displacement). The effectiveness and correct functioning of this architecture highly depends on the choice of the maximum pressure limits achievable at the delivery of the two pumps, and of the pumps displacement. The High - Low configuration differs from the Standard architecture also due to the presence of two other valves: an unloading valve (Unloading Valve) and a non-return valve (Check Valve). Table 7 shows the characteristics of the components chosen with the High-Low architecture for the case study.

Preprints (www.preprints.org) | NOT PEER-REVIEWED | Posted: 22 August 2023 doi:10.20944/preprints202308.1379.v1

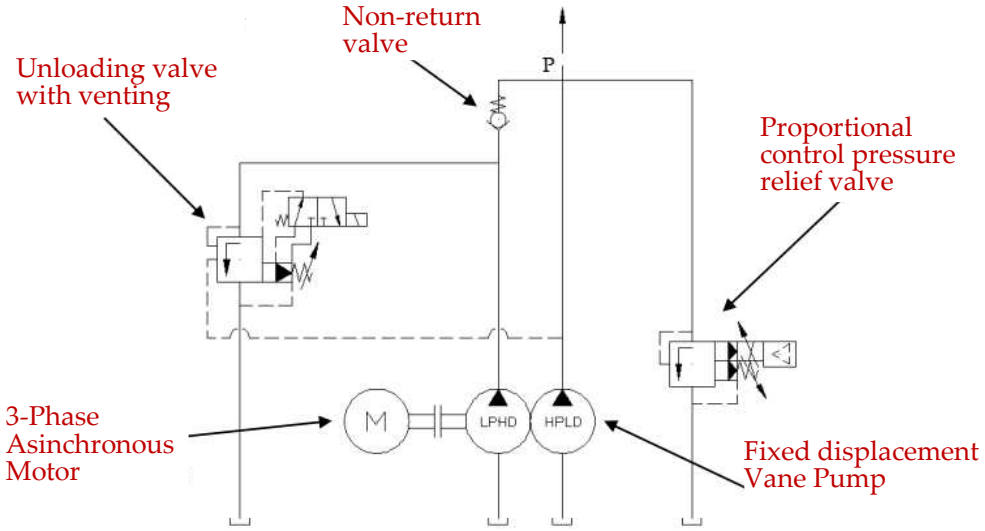

Figure 12. Circuit of the Actuation Architecture for the High-Low configuration.

From the analysis of how the system must work, it can be deduced that the shearing phase is the only one in which the flow rate that reaches the actuator is supplied only by the HPLD pump, while for the other phases both pumps contribute to supplying flow to the cylinder. The opening and closing pressure values of the drain valve must assume the values of 97.2 bar and 70 bar respectively. The High-Low configuration allows a significant reduction of the size of the electric motor (as can be seen from the comparison between the Table 7 and the Tables 6, and 5), and of the maximum pressure range, as the maximum pressure values are no longer required at the same time.

Table 7 shows the most significant technical data of the chosen components, Figure 13 the main components, and Figure 14 the active electrical power absorbed in the cycle for the High-Low Configuration.

Table 7. Designations and technical data of the main elements of the regenerative architecture.

Circuit Element	Parameter	Value
Electric motor	Code	Parker Mod. MR4P01850
	Type	4 poles - round case
	Nominal Power	18.5 [kW]
	Nominal Speed	1460 [RPM]
	Nominal Torque	121.32 [Nm]
	Efficiency	0.914
HPLD Pump	Code	Parker Mod. T7B B14
	Type	Fixed Displacement Vane Pump
	Nominal Displacement	45 [ml/min]
	Speed Range	600 - 3000 [RPM]
	Max continuous pressure	275 [bar]
LPHD Pump	Code	Parker Mod. T7ASW B40
	Type	Fixed Displacement Vane Pump
	Nominal Displacement	40 [ml/min]
	Speed Range	600 - 3000 [RPM]
	Max continuous pressure	240 [bar]
Directional Valve	Code	Parker Mod. D41FEZ32FC1NB70
	Type	Pilot operated Proportional DCV with Regeneration - A Hybrid
	Nominal flow rate	200 [l/min]
	Nominal pressure drop	5 [bar]
Pressure Relief Valve	Code	Parker Mod. R4V03535P0PM10VA1
	Type	Pilot operated proportional pressure relief valve
	Nominal flow rate	250 [l/min]
	Maximum Pressure	350 [bar]
Unloading Valve	Code	Parker Mod. R4U03 – 533
	Type	Pilot operated Unloading Valve with venting
	Nominal flow rate	150 [l/min]
	Nominal Open-Close pressure drop	28% of the setting pressure

Preprints (www.preprints.org) | NOT PEER-REVIEWED | Posted: 22 August 2023 doi:10.20944/preprints202308.1379.v1

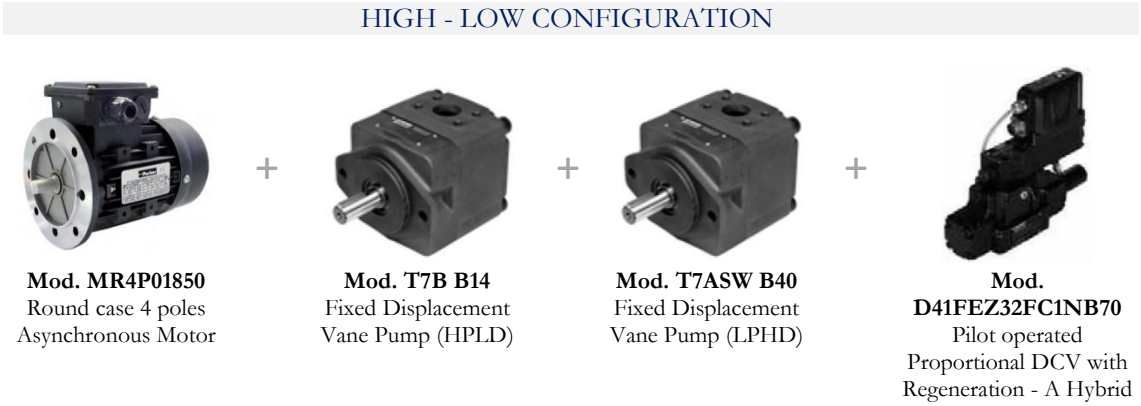

Figure 13. Main components of High - Low Configuration.

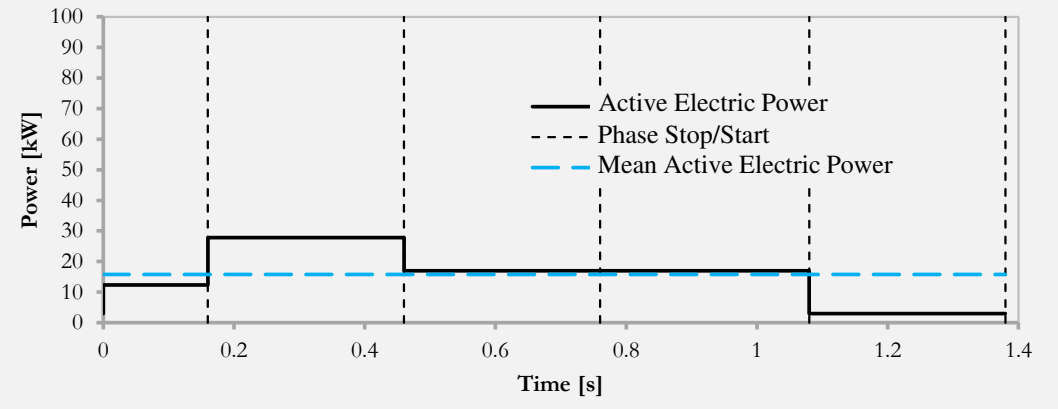

Figure 14. High Low Configuration - Active electrical power absorbed over the work cycle: instantaneous value and average value.

2.5. VDP Configuration

The VDP configuration has the same elements as the regenerative configuration except for the pump, which is of the variable displacement type. In the case study an axial piston pump is considered. There are multiple control configurations applicable to a variable displacement piston pump, which allows adjustment of the theoretical flow rate delivered by the pump during operation. Among those available, it is necessary to select the configuration that best lends itself to a comparison direct with the configurations considered in this analysis. The discussion will refer to a Proportional Displacement Control with Closed Loop Pressure Control (Figure 15).

Preprints (www.preprints.org) | NOT PEER-REVIEWED | Posted: 22 August 2023 doi:10.20944/preprints202308.1379.v1

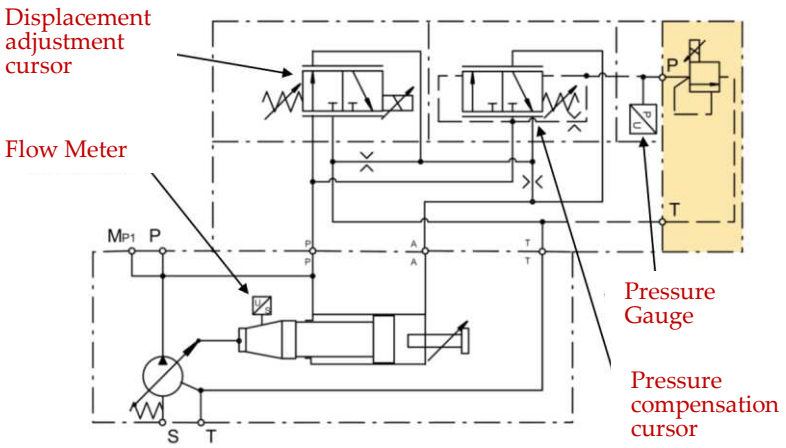

Figure 15. VDP configuration: Proportional Displacement Control with Closed Loop Pressure Control.

The main components of the VDP configuration are reported in Table 8, with their main features.

Table 8. Designations and technical data of the main elements of the regenerative architecture.

Circuit Element	Parameter	Value
Electric motor	Code	Parker Mod. MR4P01850
	Type	4 poles - round case
	Nominal Power	18.5 [kW]
	Nominal Speed	1460 [RPM]
	Nominal Torque	121.32 [Nm]
	Efficiency	0.914
Pump	Code	Parker Mod. PV 092
	Type	Axial Piston Pump - variable displacement
	Max Displacement	92 [ml/min]
	Speed Range	400 - 2500 [RPM]
	Nominal pressure	350 [bar]
Directional Valve	Code	Parker Mod. D41FEZ32FC1NB70
	Type	Pilot operated Proportional DCV with Regeneration - A Hybrid
	Nominal flow rate	200 [l/min]
	Nominal pressure drop	5 [bar]
Pressure Relief Valve	Code	Parker Mod. R4V03535P0PM10VA1
	Type	Pilot operated proportional pressure relief valve
	Nominal flow rate	250 [l/min]
	Maximum Pressure	350 [bar]

Figure 16 shows the main components, and Figure 17 the active electrical power absorbed in the cycle for the VDP Configuration.

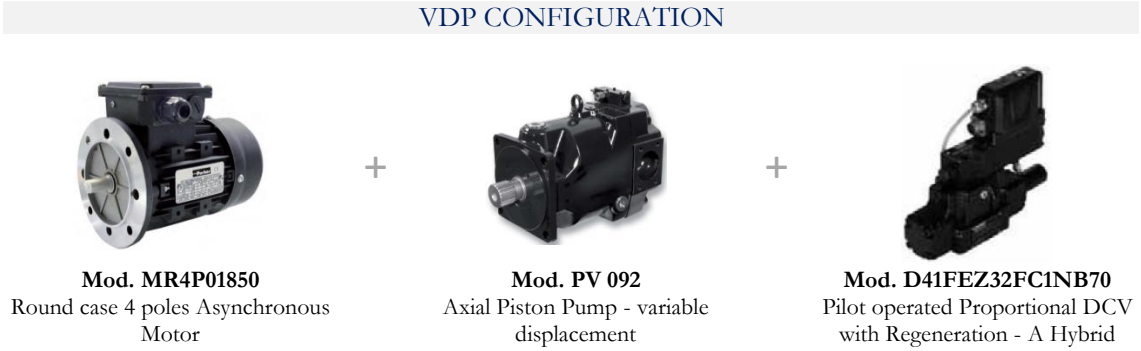

Figure 16. Main components of VDP Configuration.

Preprints (www.preprints.org) | NOT PEER-REVIEWED | Posted: 22 August 2023 doi:10.20944/preprints202308.1379.v1

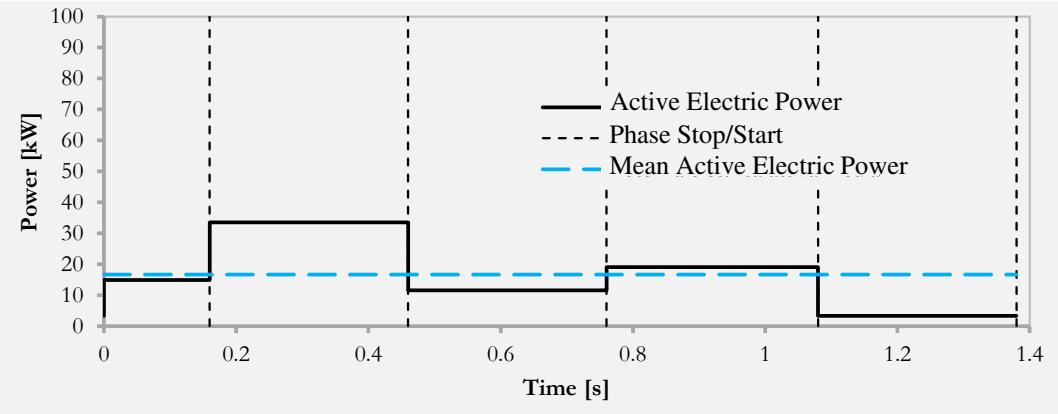

Figure 17. VDP Configuration - Active electrical power absorbed over the work cycle: instantaneous value and average value.

2.6. DCP Configuration

In this configuration, a square case three-phase asynchronous motor is connected to the power supply network by means of an alternating current frequency converter (Inverter) and the regulation of the motor speed is carried out with a vector control, while the pump is of the fixed displacement type (Figure 18). As in the case of the VDP, with the DCP configuration it is possible to adapt the flow rate delivered by the pump to the needs of the actuator. In this case, however, the displacement is fixed while the rotation speed is varied. While in the previous configurations the speed of the electric motor varies little around the nominal speed (there are only oscillations caused by the phenomenon of motion irregularity associated with the cyclic and periodic load), in this architecture the asynchronous motor varies considerably its own speed. rotation. The transition from one rotation speed to another occurs with acceleration or deceleration ramps that produce non-negligible inertia torques and consequently the profile of the flow rate required by the actuator and the desired pressure at the pump delivery is very different from what characterizes the previously considered architectures. Therefore, two sizing procedures are carried out: in a first phase the inertial actions are neglected, then they are included in the calculations, in order to verify what their real contribution is and if they have a very significant impact on consumption.

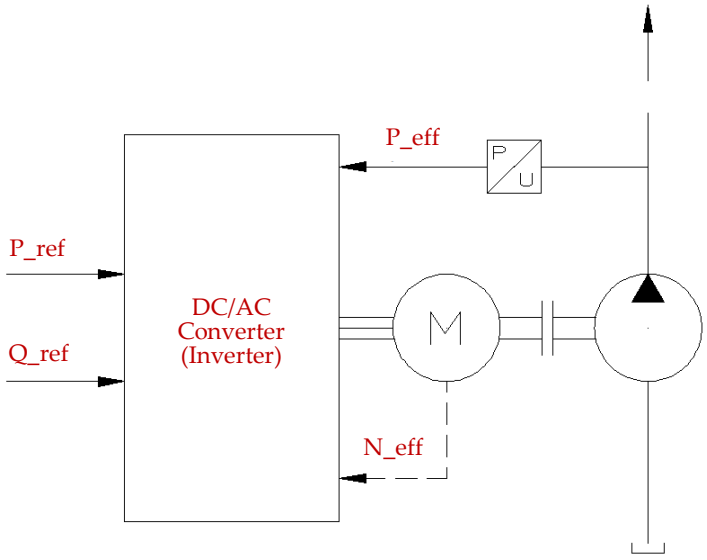

Figure 18. Direct Pump Control Architecture: power source scheme.

Preprints (www.preprints.org) | NOT PEER-REVIEWED | Posted: 22 August 2023 doi:10.20944/preprints202308.1379.v1

2.6.1. DCP Configuration-Static Sizing

The chosen pump is of the fixed displacement vane type suitable for variable speed drives, and must be sized under the constraint that the permitted speed range allows to guarantee the minimum and maximum flow rate required by the cylinder. Table 9 contains the technical data of the system components for the DCP configuration. For the asynchronous motor, in this case, it is advisable to use a different type compared to the previous configurations, i.e. a Square Frame Asynchronous Motor, because although at the electromechanical level there are no significant differences compared to a round case asynchronous motor, the inertia is greatly reduced.

Table 9 shows the most significant technical data of the chosen components, Figure 19 the main components, and Figure 20 the active electrical power absorbed in the cycle for the DCP static Configuration.

Table 9. Designations and technical data of the main elements of the regenerative architecture.

Circuit Element	Parameter	Value
Electric motor	Code	Parker Mod. MS54133KFA
	Type	4 poles - square case
	Nominal Power	16 [kW]
	Nominal Speed	1500 [RPM]
	Nominal Torque	102 [Nm]
	Efficiency	0.85
Frequency converter	Code	Parker Mod. 31V - 4G0045
	Nominal Electric Power	22 [kW]
	Nominal Current	45 [A]
	Maximum Current	49.5 [A]
	Efficiency	0.98
Pump	Code	Parker Mod. T7B E12
	Type	Fixed Displacement Vane Pump for variable speed drives
	Max Displacement	41 [ml/min]
	Speed Range	300 - 3000 [RPM]
	Nominal pressure	275 [bar]
Directional Valve	Code	Parker Mod. D41FEZ32FC1NB70
	Type	Pilot operated Proportional DCV with Regeneration - A Hybrid
	Nominal flow rate	200 [l/min]
	Nominal pressure drop	5 [bar]
Pressure Relief Valve	Code	Parker Mod. R4V03535P0PM10VA1
	Type	Pilot operated proportional pressure relief valve
	Nominal flow rate	250 [l/min]
	Maximum Pressure	350 [bar]

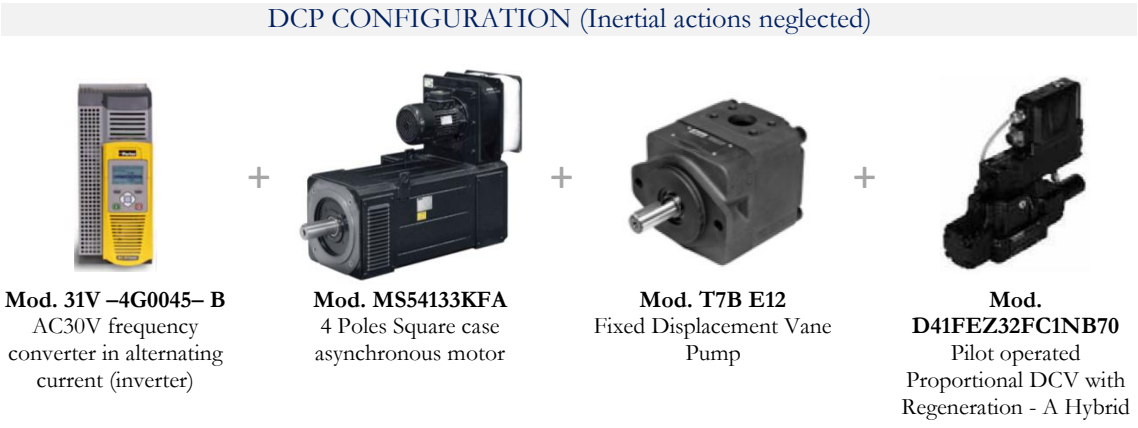

Figure 19. Main components of DCP Static Configuration.

Preprints (www.preprints.org) | NOT PEER-REVIEWED | Posted: 22 August 2023 doi:10.20944/preprints202308.1379.v1

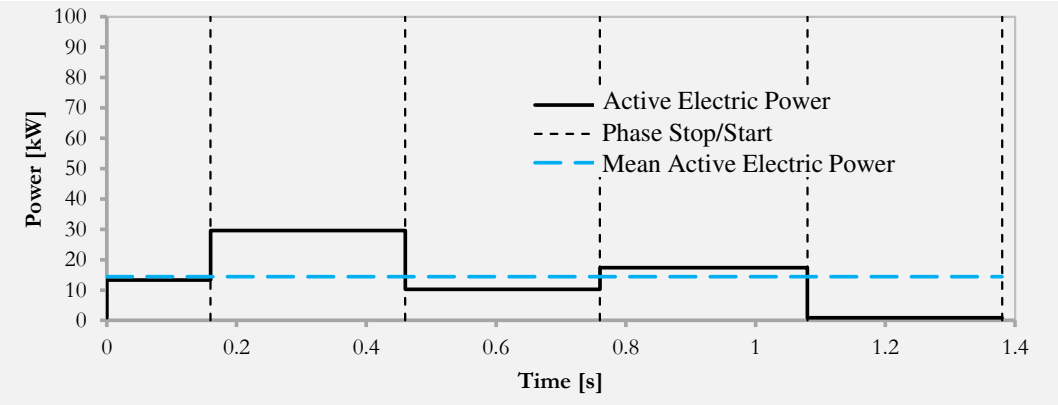

Figure 20. DCP Static Configuration- Active electrical power absorbed over the work cycle: instantaneous value and average value.

2.6.2. DCP Configuration-Dynamic Sizing

Proceeding with the sizing considering also the contribution of the inertial torques, the size of the pump and converter (Table 10) varies with respect to the simplified case (Table 9) in which they have been neglected. Conversely, the size of the electric motor does not change.

Table 10. Designations and technical data of the main elements of the regenerative architecture.

Circuit Element	Parameter	Value
Electric motor	Code	Parker Mod. MS54133KFA
	Type	4 poles - square case
	Nominal Power	16 [kW]
	Nominal Speed	1500 [RPM]
	Nominal Torque	102 [Nm]
	Efficiency	0.85
Frequency converter	Code	Parker Mod. 31V – 4G0060
	Nominal Electric Power	30 [kW]
	Nominal Current	60 [A]
	Maximum Current	66 [A]
	Efficiency	0.98
Pump	Code	Parker Mod. Mod. T7B E15
	Type	Fixed Displacement Vane Pump for variable speed drives
	Max Displacement	50 [ml/min]
	Speed Range	300 - 2700 [RPM]
	Nominal pressure	240 [bar]
Directional Valve	Code	Parker Mod. D41FEZ32FC1NB70
	Type	Pilot operated Proportional DCV with Regeneration - A Hybrid
	Nominal flow rate	200 [l/min]
	Nominal pressure drop	5 [bar]
Pressure Relief Valve	Code	Parker Mod. R4V03535P0PM10VA1
	Type	Pilot operated proportional pressure relief valve
	Nominal flow rate	250 [l/min]
	Maximum Pressure	350 [bar]

Figure 21 the main components, and Figure 22 the active electrical power absorbed in the cycle for the DCP dynamic Configuration.

Preprints (www.preprints.org) | NOT PEER-REVIEWED | Posted: 22 August 2023 doi:10.20944/preprints202308.1379.v1

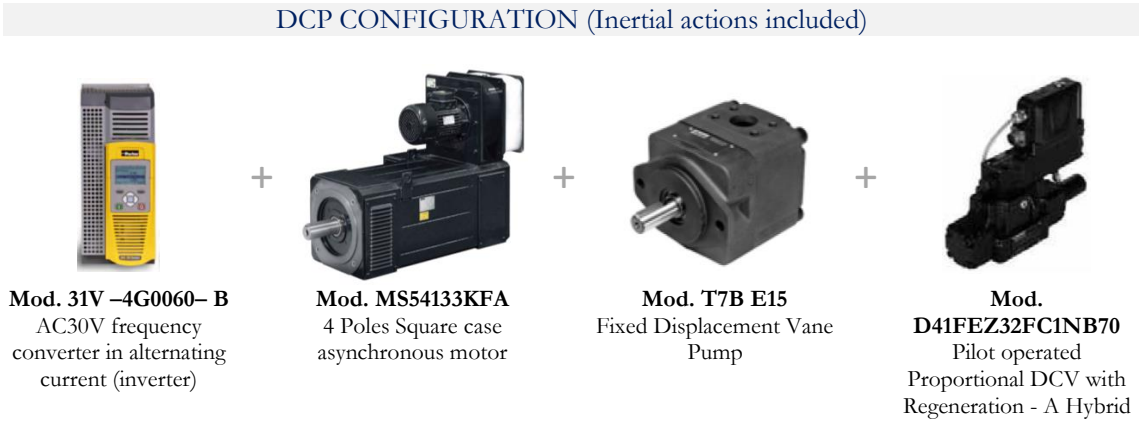

Figure 21. Main components of DCP dynamic Configuration.

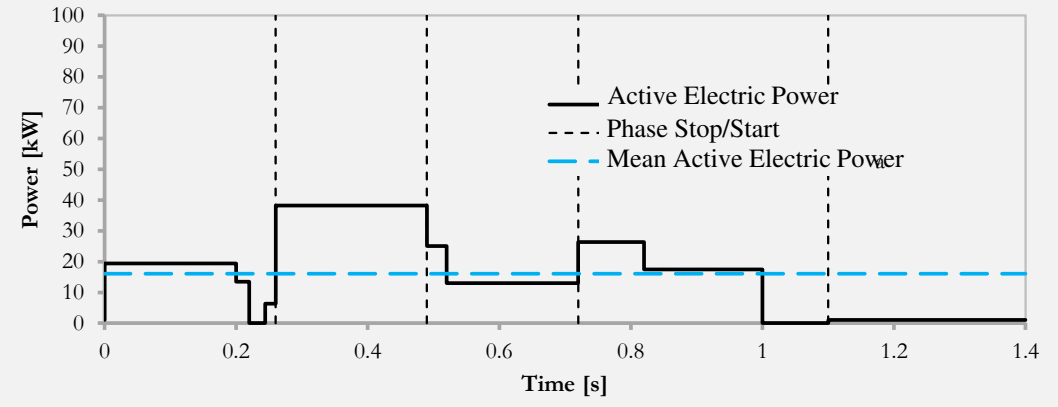

Figure 22. DCP dynamic Configuration- Active electrical power absorbed over the work cycle: instantaneous value and average value.

3. Results

3.1. Estimated Absorbed Power for the Considered Architectures

For Standard, Regenerative, High-Low and VPD plant architectures the inertial actions can typically be neglected, instead this is not the case for the architecture with DCP. In the first four architectures, the angular acceleration or deceleration ramps experienced by the induction motor during operation are caused by the phenomenon of irregularity of motion. As a result of cyclic and periodic load (the pumping unit motion), the rotational speed of the electric motor oscillates in a neighborhood typically very small, centered on the nominal rotational speed. The inertial torques resulting from this generally do not appreciably change the active electrical power absorption data summarized in Table 11, reported in detail for each individual motion phase and for each architecture considered. In Figure 23 the average values on the duty cycle for each architecture considered are diagrammed with histograms for a more effective visual comparison. An analysis was then carried out for both the static and dynamic cases for the case with DCP, and the estimated electric active power absorption data referring to the architectures with DCP show that taking into account the dynamics the estimated average active power absorbed is 1.63 kW higher. This obviously non-negligible difference is determined by the presence during operation of the architecture with DCP of very strong dynamic effects. For this system architecture, the fluctuations in speed of motor rotation are very large (even on the order of 1000 RPM) and, in the application under consideration, typically occur in times on the order of a fraction of a second. For the architectures that do not use a DCP, the motor speed fluctuations are instead on the order of 10 RPM.

Preprints (www.preprints.org) | NOT PEER-REVIEWED | Posted: 22 August 2023 doi:10.20944/preprints202308.1379.v1

Table 11. Active and reactive power absorbed in the cycle phases.

Configuration	Cycle phase	Active Power [kW]	Reactive Power [VAr]	Mean Active Power [kW]	Mean Reactive Power [VAr]
Standard	QD	24.32	21.92	40.48	29.06
	B	93.36	52.92		
	E	32.69	23.44		
	QR	32.69	23.44		
	TR	12.33	20.63		
Regenerative	QD	12.4	12.44	20.05	15.60
	B	48.39	26.14		
	E	16.59	13.07		
	QR	16.59	13.07		
	TR	3.07	11.97		
High-Low	QD	12.37	9.81	15.77	11.72
	B	27.82	16.97		
	E	16.99	11.23		
	QR	16.99	11.23		
	TR	2.99	8.52		
VDP	QD	14.85	10.5	16.67	12.71
	B	33.56	21.87		
	E	11.53	9.62		
	QR	19.04	12.03		
	TR	3.35	8.55		
DCP Static	QD	12.86	24.54	14.43	16.49
	B	29.18	22.29		
	E	9.83	9.29		
	QR	16.91	28.05		
	TR	0.44	1.27		
DCP Dynamic	QD Acc1	2.34	1.6	16.06	21.26
	QD Acc2	35.25	48.47		
	QD Unif	12.9	20.63		
	QD Dec1	-25	41.62		
	QD Dec2	11.44	11.58		
	QD Acc2	35.25	48.47		
	B	37.58	46.75		
	E	12.41	11.74		
	QR Acc1	21.66	16.89		
	QR Acc2	29.9	44.49		
	QR Unif	16.91	22.76		
	QR Dec1	-24.22	34.42		
	QR Dec2	-3.19	2.15		
	TR	0.44	1.05		

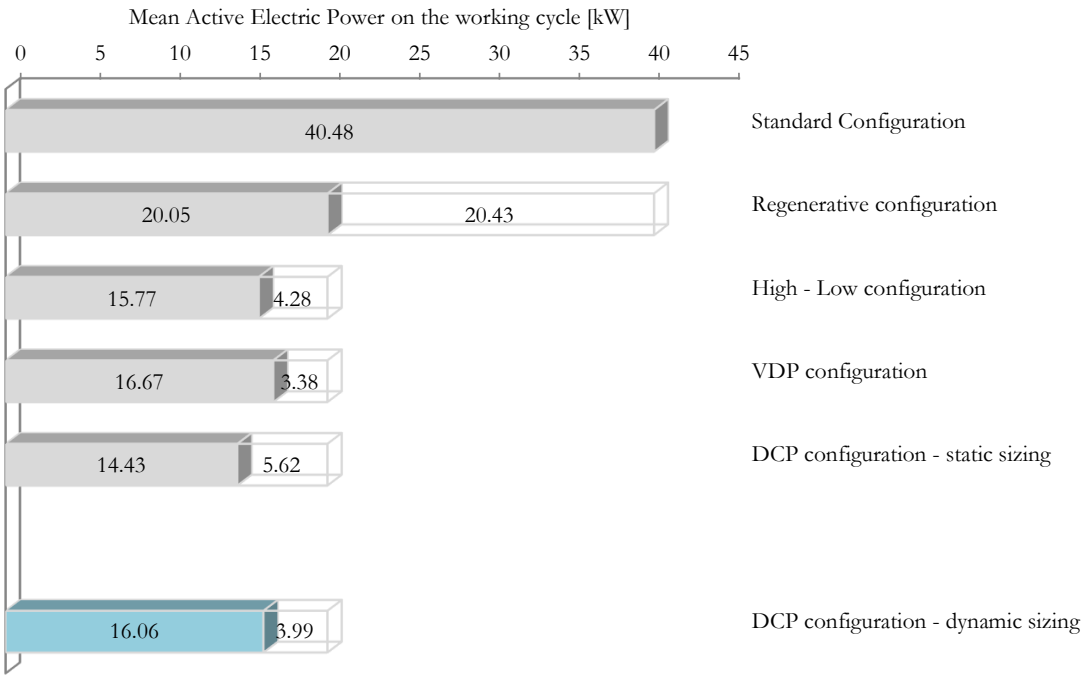

Figure 23. Comparison between the different plant architectures in terms of average active electrical power absorption during the work cycle.

Preprints (www.preprints.org) | NOT PEER-REVIEWED | Posted: 22 August 2023 doi:10.20944/preprints202308.1379.v1

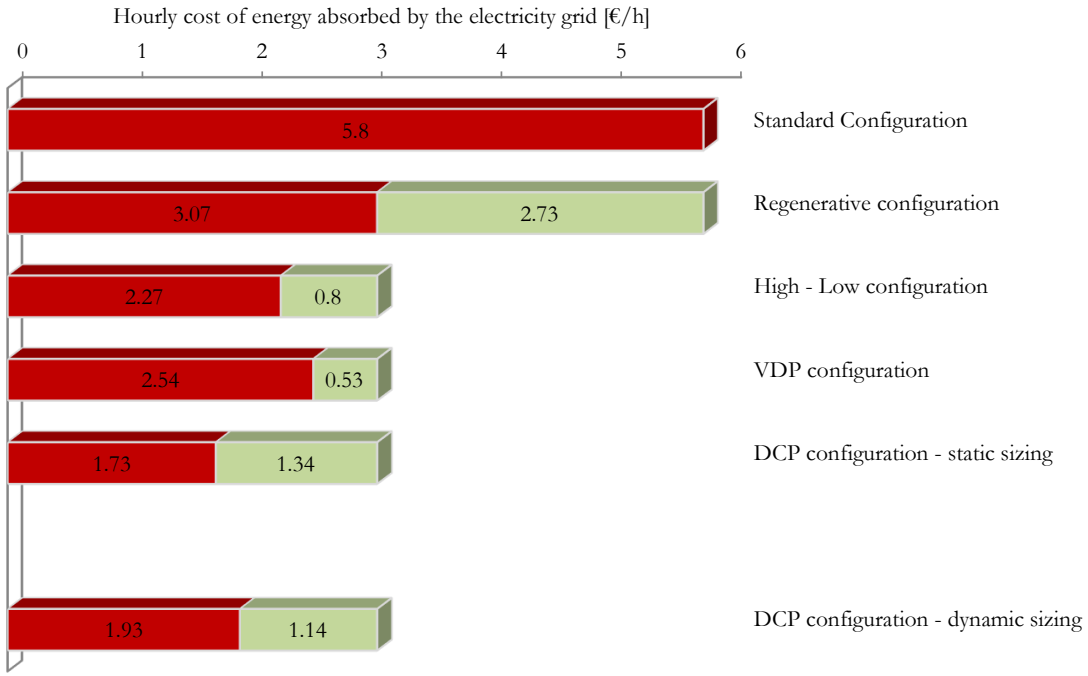

Figure 24. Comparison between the different system architectures in terms of the hourly cost of electricity absorbed (active and reactive) during the work cycle.

The matrix in Table 12 shows the percentage variation between the average active power required by one architecture (in the rows) versus another (in the columns), in Table 13 a similar comparison is reported for absorbed reactive power, and in Table 14for the hourly cost of absorbing electricity from the power supply grid.

Table 12. Comparison in percentage terms of active power absorbed with the different configurations.

	Standard	Regenerative	High-Low	VDP	DCP-static
Regenerative	-50.5%				
High - Low	-61.1%	-21.3%			
VDP	-58.8%	-16.8%	+5.7%		
DCP-static	-64.3%	-28.1%	-8.4%	-13.4%	
DCP-dynamic	-60.3%	-19.9%	+1.8%	-3.6%	+11.2%

Table 13. Comparison in percentage terms of reactive power absorbed with the different configurations.

	Standard	Regenerative	High-Low	VDP	DCP-static
Regenerative	-46.3%				
High - Low	-59.7%	-24.8%			
VDP	-56.3%	-18.5%	+8.4%		
DCP-static	-43.2%	+5.7%	+40.6%	+29.6%	
DCP-dynamic	-26.8%	+36.2%	+81.3%	+67.1%	+28.9%

Table 14. Comparison in percentage terms of the hourly cost of absorbing electricity from the power supply grid between the different configurations (based on Italian energy market rules).

	Standard	Regenerative	High-Low	VDP	DCP-static
Regenerative	-47.1%				
High - Low	-60.8%	-26.1%			
VDP	-56.2%	-17.3%	+11.9%		
DCP-static	-70.1%	-43.7%	-23.8%	-31.9%	
DCP-dynamic	-66.7%	-37.1%	-15.1%	-24%	+11.5%

Preprints (www.preprints.org) | NOT PEER-REVIEWED | Posted: 22 August 2023 doi:10.20944/preprints202308.1379.v1

3.2. Experimental Results

Figure 25 reports the results of experimental measurements conducted on the plant in which the architecture with DCP was implemented. More specifically, Figure 25.a reports the profile of the absorbed current by a phase; Figure 25.b reports the electrical active power absorbed by the frequency converter. The average value of the experimentally measured active electric power is 14.85 kW.

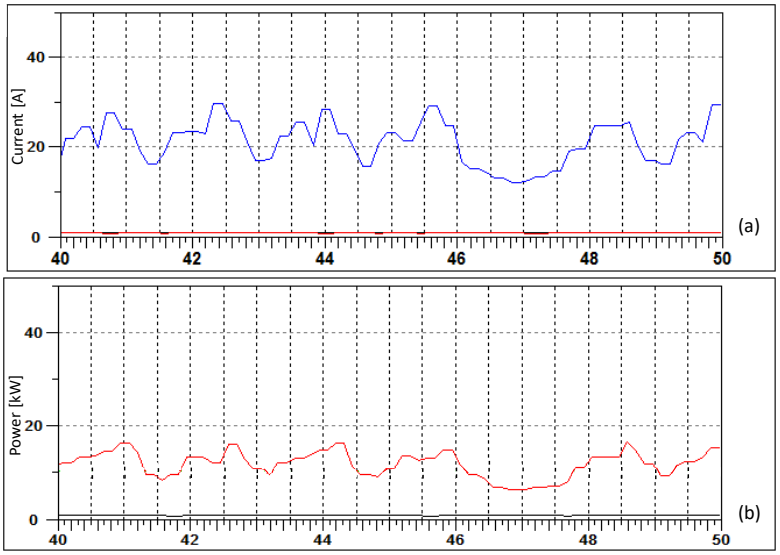

(a) Active electrical current absorbed [A] by the architecture with DCP over time [s]. The measurement is made upstream of the frequency converter and is related to a single phase. To get the total current just multiply by √3.

(b) Active electrical power absorbed [kW] by the architecture with DCP over time [s]. The measurement is made upstream of the frequency converter.

Figure 25. Active current and active electrical power absorbed by the real blanking press with DCP power architecture.

4. Discussion

From the analysis conducted on the basis of the system modeling, the difference in active power absorbed in the case of DCP architecture neglecting dynamic aspects is underestimated of 1.63 kW compared with the case taking into account dynamic effects. The difference is significant, hence the considerations that follow consider the DCP dynamic architecture.

The adoption of regeneration in the direct control valve results in a reduction of the average active power input of 50.5%. In architectures 3, 4 and 5 regeneration is retained as a common element, so the differences that occur in the absorbed active power are determined only by the differences in the configurations.

From the results resumed in Table 12, it emerges that the High - Low, VDP and DCP solutions realize higher energy efficiency for the plant than the simply Regenerative architecture. In fact, in all three cases, there is a more or less pronounced decrease in the active electrical power absorbed from the power grid.

The solutions that achieve the greatest savings in terms of active power consumption are in order the High - Low configuration, followed by DCP, and finally VDP. The difference between the Hig-Low configuration and the DCP is very small (1.8%).

The particular efficiency of the High - Low architecture for this application is attributable to the nature of the variable-speed considered industrial process. As a matter of fact, the High-Low architecture is particularly well suited to operation with stages characterized by high oil flow rates at low pressures alternating with phases with low fluid flow rates at high pressures. Typically, this is the case of stamping. The lower energy efficiency of the solution with VDP is caused by the additional pilot oil flow rates, which must be continuously ensured to maintain the displacement regulation of the axial piston pump.

Comparing, the VDP configuration and the DCP, the latter realizes savings in terms of electrical power consumption, even if the saving is small for the considered case. Therefore, we can conclude

 doi:10.20944/preprints202308.1379.v1

that, from the point of view of the absorption of average active electric power during the work cycle, the DCP solution stands as slightly more advantageous than the VDP one, or that certainly the VDP solution does not emerge as better than the DCP one.

From data referred to the active electrical power parameter (Figure 12 and Table 12), the solution with DCP realized a marked advantage over the Standard architecture, a slight advantage over the VDP configuration, and a comparable, or even slightly lower, result than the High - Low solution.

If, on the other hand, the comparison is conducted on the cost parameter of electric power (based on the italian energy pricing), the DCP architecture comes out as clearly cheaper even against the High - Low and VDP solutions. This is due to the reactive component of the electric power (Table 13), for which economic penalties occur, in cases of high absorption of reactive electric power from the power grid. For the DCP architecture the economic penalties are not present. This is ensured by the action of the capacitor bank present in the drive, which brings the reactive (inductive) electrical energy absorbed below 50% of the active one or, equivalently, reduce the power factor above the value of 0.9. Therefore, taking into account the contributions of both active and reactive power, the most advantageous solution (among those analyzed) from the point of view of energy operating costs is the DCP, which also compared to the Hig-Low architecture results in a savings of 15%.

For the case of architecture with DCP, a comparison between the theoretical absorption of active electrical power input (16.06 kW) and the absorption actually measured on the system in a cycle (14.85 kW) is possible. An overestimation of the real figure of about 8% is observed. This value is quite small. Therefore, it can be considered that the analysis conducted reflects reality sufficiently well.

5. Conclusions

The choice of power generation architecture of a hydraulic system has a very significant impact on energy efficiency and operating costs. The comparative study of the most common hydraulic architectures, used in the driving of an industrial process with time-varying speeds and work force, highlighted the differences between the various solutions in quantitative terms, providing objective comparison data that were not available in the literature.

The modern hydraulic architecture with Drive Controlled Pump and DCV with Regeneration - A Hybrid, is, limited to the category of industrial processes exemplified, a very efficient solutions in terms of energy absorption and cost-effectiveness.

It has been verified that the dynamic phenomena, which are often overlooked during sizing, have a significant impact on overall energy absorption.

The oleo-hydraulic architectures reviewed constitute a significant part of the state of the art in the field of hydraulic technology dedicated to the actuation of industrial machines, but not its entirety. Other solutions, characterized by high levels of energy efficiency, are architecture that uses high efficiency asynchronous square-case motors, or architectures with a brushless synchronous electric motor and a pump with internal gears.

Another oleo-hydraulic architecture that could be studied, but which poorly fits the exemplified industrial process, involves the use of an accumulator installed in parallel with a fixed-displacement pump.

Furthermore, the analysis could be completed from an economic point of view by considering the analysis of the initial investment costs necessary for each considered architecture.

However, it can be concluded that energy-conscious choices for the power architecture of a hydraulic axis can benefit from the presented analysis.

Funding: This research received no external funding.

Acknowledgments: Acknowledgement of the valuable technical contribution of the engineers Davide Ceppelli, Alessandro Pennacchio and Felice Lanzetti.

Abbreviations

The following abbreviations are used in this manuscript:

ERS	energy regeneration system
SI	single-valve independent control
SMISMO	separate meter in and separate meter out control
DP	dual valve parallel control
DCP	Direct Driven Pump-controlled hydraulic system
DCV	Directional Control Valve
CDS	combined drive system
HIMMs	hydraulic injection molding machines
FC	force control
EHVDPS	electro-hydraulic variable-displacement pump system
LSC	load-sensing control
CSPC	constant supply pressure control
VDP	Variable Displacement Pump
QD	Quick Descent
B	Blanking
E	Expulsion
QR	Quick Rise
TR	Table Rotation

References

1. Lin, T.; Chen, Q.; Ren, H.; Huang, W.; Chen, Q.; Fu, S. Review of boom potential energy regeneration technology for hydraulic construction machinery. *Renewable and Sustainable Energy Reviews* **2017**, *79*, 358–371. https://doi.org/https://doi.org/10.1016/j.rser.2017.05.131.
2. Ho, T.H.; Le, T.D. Development and Evaluation of Energy-Saving Electro-Hydraulic Actuator. *Actuators* **2021**, *10*. https://doi.org/10.3390/act10110302.
3. Niu, S.; Wang, J.; Zhao, J.; Shen, W.; Yang, J. A Novel Multifunctional Energy-saving Electro-hydraulic Servo System. In Proceedings of the 2021 IEEE/ASME International Conference on Advanced Intelligent Mechatronics (AIM), 2021, pp. 314–319. https://doi.org/10.1109/AIM46487.2021.9517649.
4. Schmidt, L.; Hansen, K.V. Electro-Hydraulic Variable-Speed Drive Networks: Idea, Perspectives, and Energy Saving Potentials. *Energies* **2022**, *15*. https://doi.org/10.3390/en15031228.
5. Xu, Z.; Liu, Y.; Hua, L.; Zhao, X.; Guo, W. Energy analysis and optimization of main hydraulic system in 10000 kN fine blanking press with simulation and experimental methods. *Energy Conversion and Management* **2019**, *181*, 143–158. https://doi.org/https://doi.org/10.1016/j.enconman.2018.12.012.
6. Zhao, K.; Liu, Z.; Yu, S.; Li, X.; Huang, H.; Li, B. Analytical energy dissipation in large and medium-sized hydraulic press. *Journal of Cleaner Production* **2015**, *103*, 908–915. Carbon Emissions Reduction: Policies, Technologies, Monitoring, Assessment and Modeling, https://doi.org/https://doi.org/10.1016/j.jclepro.2014.03.093.
7. Li, L.; Huang, H.; Zhao, F.; Sutherland, J.W.; Liu, Z. An Energy-Saving Method by Balancing the Load of Operations for Hydraulic Press. *IEEE/ASME Transactions on Mechatronics* **2017**, *22*, 2673–2683. https://doi.org/10.1109/TMECH.2017.2759228.
8. Koitto, T.; Calonius, O.; Kauranne, H.; Minav, T.; Pietola, M. Enhanced energy efficiency of industrial application by direct driven hydraulic unit. In Proceedings of the 2018 Global Fluid Power Society PhD Symposium (GFPS), 2018, pp. 1–6. https://doi.org/10.1109/GFPS.2018.8472365.
9. Chiang, M.H., Y.Y.Y.Y.C.Y. Integrated control of clamping force and energy-saving in hydraulic injection moulding machines using decoupling fuzzy sliding-mode control. *The International Journal of Advanced Manufacturing Technology* **2005**, *27*, 2673–2683. https://doi.org/10.1007/s00170-004-2138-z.
10. Teguede, A.; Kamsu-foguem, B.; Houe, R. Advances in Engineering Software Health condition monitoring of a complex hydraulic system using Deep Neural Network and DeepSHAP explainable XAI. *Advances in Engineering Software* **2023**, *175*, 103339. https://doi.org/10.1016/j.advengsoft.2022.103339.
11. Tiboni, M.; Incerti, G.; Remino, C.; Lancini, M. Comparison of signal processing techniques for condition monitoring based on artificial neural networks. *Applied Condition Monitoring* **2019**, *15*, 179–188. https://doi.org/10.1007/978-3-030-11220-2_19.
12. Gu, L.; Shi, Y. Online Monitoring Technique of Power Condition for Inverter-Fed Motor Driven Hydraulic System **2019**. *2019*. https://doi.org/10.1155/2019/4908942.

13. Tiboni, M.; Remino, C. Condition monitoring of a mechanical indexing system with artificial neural networks. In Proceedings of the WCCM 2017 - 1st World Congress on Condition Monitoring 2017, 2017.
14. Makansi, F.; Schmitz, K. Data-Driven Condition Monitoring of a Hydraulic Press Using Supervised Learning and Neural Networks. *Energies* **2022**, *15*. https://doi.org/10.3390/en15176217.
15. Rydberg, K.E. Energy Efficient Hydraulics – System solutions for loss minimization. In Proceedings of the National Conference on Fluid Power, Linköping University, Linköping, Sweden, 16 - 17 March, 2015, 2015, pp. 16–17.